KfK 4911
September 1991

Tests of the $^{238}U + n$ Evaluation for JEF-2 in the Unresolved Resonance Region

F. H. Fröhner
Institut für Neutronenphysik und Reaktortechnik
Projekt Nukleare Sicherheitsforschung

Kernforschungszentrum Karlsruhe

KERNFORSCHUNGSZENTRUM KARLSRUHE
Institut für Neutronenphysik und Reaktortechnik
Projekt Nukleare Sicherheitsforschung

KfK 4911

TESTS OF THE $^{238}U+n$ EVALUATION FOR JEF-2 IN THE UNRESOLVED RESONANCE REGION

F.H. Fröhner

Kernforschungszentrum Karlsruhe GmbH, Karlsruhe

Kernforschungszentrum Karlsruhe GmbH
Postfach 3640, 7500 Karlsruhe 1

ISSN 0303-4003

TESTS DER $^{238}U + n$-AUSWERTUNG FÜR JEF-2 IM NICHT AUFGELÖSTEN RESONANZBEREICH

ZUSAMMENFASSUNG

Während der Testphase der Kerndatenbibliothek JEF-2 wurde die Neuauswertung von Wirkungsquerschnitten für $^{238}U + n$ im nicht aufgelösten Resonanzbereich anhand von neuen Messungen von Einfangquerschnitten, von Transmissionsmessungen mit dicken Proben und von Selbstindikations-Quotienten überprüft. (Die Neuauswertung ist von 10 keV bis 200 keV in JEF-2, bis 149 keV in ENDF/B-VI aufgenommen.) Auswirkungen der nicht aufgelösten Resonanzstruktur auf Selbstabschirmung und Vielfachstreuung wurden mit Monte-Carlo-Methoden behandelt auf der Grundlage von Niveaustatistik und mittleren Resonanzparametern. Dabei ergab sich, daß man mit den mittleren Wirkungsquerschnitten und den mittleren Resonanzparametern der Neuauswertung alle Testdaten sehr befriedigend wiedergeben kann. Der resonanzgemittelte Einfangquerschnitt unterhalb von 200 keV ist nun anscheinend mit rund 2 % Unsicherheit bekannt.

TESTS OF THE $^{238}U + n$ EVALUATION FOR JEF-2 IN THE UNRESOLVED RESONANCE REGION

ABSTRACT

During the JEF-2 test phase the new evaluation for $^{238}U + n$ in the unresolved resonance region (adopted for JEF-2 up to 200 keV, for ENDF/B-VI up to 149 keV) has been checked against recent capture cross section measurements and against thick-sample transmission data and capture self-indication ratios. Effects of the unresolved resonance structure on self-shielding and multiple scattering were treated by Monte Carlo techniques based on resonance statistics and average resonance parameters. It was found that the average cross sections and the average resonance parameters given in the new evaluation permit very satisfactory reproduction of all the test data. The resonance-averaged capture cross sections below 200 keV appear now to be known with roughly 2 % uncertainty.

Tests of the ^{238}U+n Evaluation for JEF-2 in the Unresolved Resonance Region

F.H. Fröhner
Kernforschungszentrum Karlsruhe
Institut für Neutronenphysik und Reaktortechnik
Postfach 3640, W-7500 Karlsruhe 1
Germany

ABSTRACT. During the JEF-2 test phase the new evaluation for ^{238}U + n in the unresolved resonance region (adopted for JEF-2 up to 200 keV, for ENDF/B-VI up to 149 keV) has been checked against recent capture cross section measurements and against thick-sample transmission data and capture self-indication ratios. Effects of the unresolved resonance structure on self-shielding and multiple scattering were treated by Monte Carlo techniques based on resonance statistics and average resonance parameters. It was found that the average cross sections and the average resonance parameters given in the new evaluation permit very satisfactory reproduction of all the test data. The resonance-averaged capture cross sections below 200 keV appear now to be known with roughly 2 % uncertainty.

1. Introduction

At present the cross section resonances of ^{238}U+n have been resolved and analysed up to 10 keV (Moxon et al. 1989). The resonance structure of the ^{238}U neutron cross sections persists, of course, also above 10 keV but resonance overlap increases and instrumental resolution deteriorates with growing neutron energy. The resonance structure at higher energies is therefore unresolved or at best partially resolved in the available experimental data. Now any resonance structure, whether resolved or not, causes phenomena such as resonance self-shielding and temperature-dependent resonance absorption, effects that are not only essential for the correct extraction of average total and capture cross sections from experimental resonance-averaged transmission and capture yield data, but also crucial for questions of reactor safety, e. g. about the temperatur dependence of the reactivity (Doppler coefficient). The effects of unobserved resonances become unimportant only above roughly 150 to 200 keV for ^{238}U.

Modern evaluated nuclear data files contain, therefore, not only average point cross sections for the unresolved resonance region but also average resonance parameters characterising the resonance structure. These are mean level spacings and average partial widths for all energetically allowed reactions (elastic scattering, radiative capture, fission, etc.) and for all relevant level spins and parities. Potential scattering including the influence of distant levels is given in the form of effective nuclear radii. These parameters belong to level-statistical "laws" (Dyson-Mehta statistics or the more approximate Wigner distribution of level spacings, and the Porter-Thomas distribution of partial widths, see e. g. Porter

1965) that allow computation of the effects of unknown resonances at least probabilistically, as averages (expectation values) over the resonance parameter distributions. Rigorous analytical averaging is extremely difficult and has so far been achieved only in the relatively simple case of resonance-averaged cross sections for zero temperature (Verbaarschot, Weidenmüller and Zirnbauer 1985). If temperature-dependent cross section functionals like average transmission or self-indication ratios are to be calculated rigorously it is simpler to resort to Monte Carlo sampling of resonance "ladders".

In a recent evaluation of ^{238}U + n (Fröhner 1989) the unresolved resonance region was taken to extend from 10 keV to 300 keV. The evaluation is based on simultaneous statistical-model (Hauser-Feshbach) fits to a large body of total, capture and inelastic-scattering cross section data, with rigorous (Bayesian) inclusion of a-priori information from the resolved resonances below 10 keV and from optical-model fits above 300 keV. It has been adopted up to 200 keV for JEF-2 (see Nordborg et al. 1991), up to 149 keV for ENDF/B-VI (see Kanda 1991), hence the test results to be reported here are relevant both to the JEF-2 library up to 200 keV and to ENDF/B-VI up to 149 keV. The tests made use of microscopic data that had not been considered yet in the evaluation: (i) The JEF-2 point data were compared with new capture data, (ii) both the JEF-2 point data and the JEF-2 average resonance parameters were used as input in Monte Carlo calculations of thick-sample transmission and self-indication ratios and compared with the large available data base of these quantities. The results are reported below, but it is appropriate to discuss first the consistency between the point data and the average resonance parameters given in the new ^{238}U file.

2. Consistency Between Evaluated Average Cross Sections and Evaluated Average Resonance Parameters.

If point cross sections are given together with average resonance parameters, as in the new evaluation of the unresolved region of ^{238}U + n, there is always the question of consistency between the two. In the present case the evaluated point cross sections were generated at the same time as the evaluated average resonance parameters by a cross section fitting program (FITACS, see Fröhner 1989) which uses Hauser-Feshbach theory (the level-statistical model of compound-nuclear reactions) in a form that is more sophisticated than the single-level Breit-Wigner treatment allowed by current ENDF format rules for the unresolved resonance region, and implemented in processing codes for ENDF-formatted evaluated files. Differences exist, for instance, with respect to the treatment of width fluctuation corrections, the use of effective nuclear radii, and the number of inelastic channels admitted. It is therefore not to be expected that ENDF-type processing codes such as NJOY (see MacFarlane 1989) calculate exactly the same average cross sections as FITACS does from given parameters. The average resonance parameters for the final FITACS calculation have been presented (Fröhner 1989, Table II) for zero neutron energy. The full energy dependence of the mean level spacings and the average reduced neutron widths for s-, p- and d-wave levels, as stored in JEF-2, is shown in Figs. 1 and 2. (The average radiation widths increase almost linearly by about 9.4 % between 0 and 200 keV.) Fig. 3 shows that the NJOY-generated average cross sections differ at most by about 1.5 % from the FITACS-generated recommended values except above the second (4+) inelastic threshold at 149 keV where the ENDF restriction to one inelastic ("residual") width begins to hurt. The point cross sections and the average resonance parameters coexisting in the file are thus reasonably consistent with respect to NJOY calculations. Nevertheless, as a matter

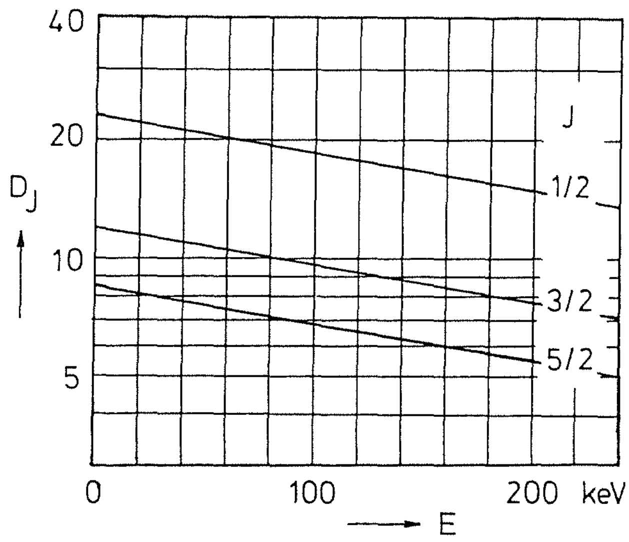

Fig. 1. Energy dependence of the mean level spacings given in JEF-2. The nearly exponential decrease with energy, typical for Fermi gas nuclear models, is due to the composite level density formula of Gilbert and Cameron (1965) that was employed in the Hauser-Feshbach fits.

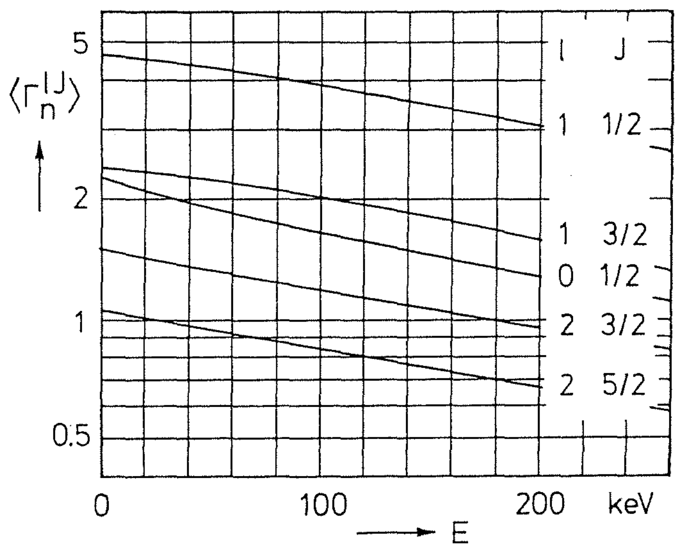

Fig. 2. Energy dependence of the average reduced neutron widths given in JEF-2. Note its similarity with that of the mean level spacings in Fig. 1 which implies nearly constant neutron strength functions, $S_l = \langle\Gamma_n^{lJ}\rangle/D_J$, in this energy range.

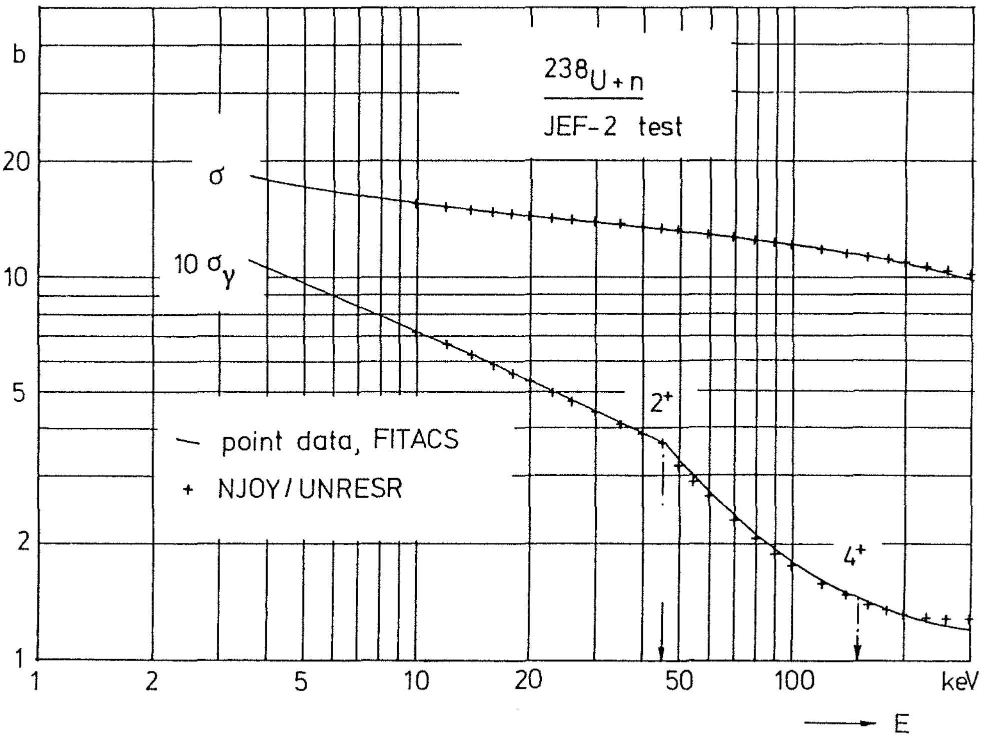

Fig. 3. Comparison of recommended average total and capture cross sections (curves, through JEF-2 point data) with cross sections (crosses) calculated with the NJOY Nuclear Data Processing System from the average resonance parameters given in JEF-2 for self-shielding calculations.

of principle, and as indicated by a flag in the JEF-2 file, the average resonance parameters are to be used only for the calculation of self-shielding (Bondarenko) factors, or for the sampling of resonance ladders in Monte Carlo calculations, whereas average cross sections (for infinite dilution) are to be obtained by interpolation between the point cross sections given in the file.

3. Comparison with Recent Capture Data

After the JEF-2 evaluation of the ^{238}U neutron cross sections had been completed new capture yield data were reported by Macklin et al. (1988). These data show partially resolved resonance structure, and they are systematically higher than the JEF-2 average capture cross section, as Fig. 4 shows. Now the directly observable capture yield divided by the sample thickness cannot simply be equated to the capture cross section except in the limit of vanishing sample thickness. For practical sample thicknesses the yield is always affected by self-shielding and multiple scattering. One has

$$\langle y_\gamma \rangle = \langle \frac{1 - e^{-n\sigma}}{n\sigma} n\sigma_\gamma + y_{\gamma s} \rangle , \tag{1}$$

where y_γ is the capture yield, i. e. the probability that an incident neutron is captured in the sample, $y_{\gamma s}$ the multiple-scattering contribution, σ the (Doppler-broadened) total cross

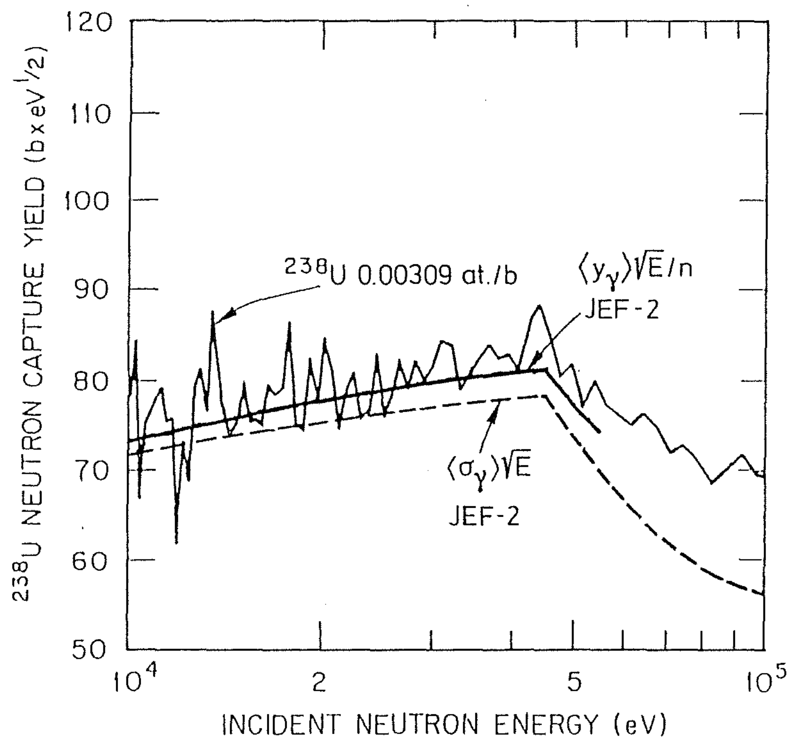

Fig. 4. High-resolution ORELA capture yields divided by sample thickness, i. e. raw capture cross sections uncorrected for resonance self-shielding and multiple scattering (fluctuating curve, from Macklin et al. 1988), recommended JEF-2 capture cross sections (broken line), and capture yields divided by sample thickness calculated with Monte Carlo techniques from JEF-2 average resonance parameters (smooth solid line), all multiplied by $\sqrt{E}$.

section, σ_γ the (Doppler-broadened) capture cross section, n the areal density of target nuclei (i. e. the sample thickness in at./b), and the angular brackets denote resolution broadening, i. e. an average over an incident-energy interval containing a statistically meaningful sample of resonances. The first term on the right, the first-collision yield, is the capture cross section times the sample thickness times a factor describing self-shielding. Self-shielding tends to lower the yield, multiple scattering tends to increase it. At low keV energies the two effects almost cancel, at higher energies there is a net enhancement.

The average capture yield is thus a functional of the total and capture cross sections, complicated by their correlated resonance structure and by multiple-collision events, with cross sections changing violently from collision to collision. An analytical calculation is possible only approximately. On the other hand Monte Carlo techniques permit high accuracy both in the sampling of resonance cross sections and in the simulation of multiple-collision events leading to eventual capture.

An updated version of a Monte Carlo program (SESH, Fröhner 1968), written for the calculation of sample-thickness corrections to resonance-averaged transmission, capture and self-indication data, was employed to calculate, from the JEF-2 average parameters, capture yields expected for the sample used by Macklin et al. The program simulates multiple-collision events, generating for each collision a "resonance environment" by sampling resonance spacings from the Wigner distribution and partial widths from Porter-Thomas distributions with the average spacings and average widths taken from the file. In this way a resonance ladder is generated whose length was chosen as eight resonances, four below and four above the energy of interest. This is done for all level sequences (level spins and parities) excited by the s-, p- and d-wave. Doppler-broadened total, capture and scattering cross sections are then calculated from the sampled resonance parameters in single-level Breit-Wigner (SLBW) approximation at the energy of interest. Resonance environments for subsequent collisions are taken as uncorrelated. This is reasonable if the average energy loss of the scattered neutron is so much larger than the mean level spacing as is the case for ^{238}U in the unresolved resonance region. The single-level approximation is adequate for a simulation of resonance effects in this energy range according to de Saussure and Perez (1973). The Monte Carlo generated average cross sections are routinely checked against the analytical SLBW expressions to make sure they agree within sampling errors (well below 1 % with the employed sample size of 100 000 neutron histories per energy point and the chosen ladder length of eight resonances). The calculated yield curve, shown as a smooth solid line in Fig. 4, is reasonably consistent with the average of the observed fluctuating capture yields, at least below the discontinuity (Wigner cusp) at the first inelastic (2+) threshold at 45 keV.

The relative shape of the evaluated average capture cross section is nicely confirmed below about 200 keV by a recent measurement with Fe and Si filtered neutron beams at 24, 55 and 146 keV reported by Kobayashi, Yamamoto and Fujita (1991).

A very accurate absolute capture cross section measurement has been announced by Quang and Knoll (1990). Using a calibrated spherical Sb-Be photo-neutron source and the manganese bath technique they obtained, essentially without reliance on any reference cross section,

$$\langle\sigma_\gamma\rangle = 494 \pm 11\,\mathrm{mb} \qquad \text{at } E = 23\,\mathrm{keV}\,.$$

The JEF-2 value at the same neutron energy, 500 mb, is in excellent agreement with this precision measurement. That is a rather direct confirmation of the absolute value of the evaluated average capture cross section, at least at relatively low keV energies, yet it does not shed much light on the correctness of the resonance structure implied by the average resonance parameters in the file. The resonance structure, however, is decisive for self-shielding in bulk material, e. g. in fission reactor fuel or in breeder blankets.

4. Comparison with Thick-Sample Transmission Data

The representation of the resonance structure can be tested by comparing cross section functionals like thick-sample transmission or capture self-indication ratios computed from the evaluated file with resonance-averaged measurements of these quantities. The transmission of a "filter" sample of thickness n (nuclei/b), averaged over a suitably broad energy interval, can be written as

$$\langle e^{-n\sigma}\rangle = e^{-n\langle\sigma\rangle}\left(1 + \frac{n^2}{2}\,\mathrm{var}\,\sigma - + \ldots\right)\,, \qquad (2)$$

where the variance, var $\sigma = \langle(\sigma - \langle\sigma\rangle)^2\rangle$, and higher moments of the total cross section distribution indicate how pronounced the resonance structure is. The relevant parameters

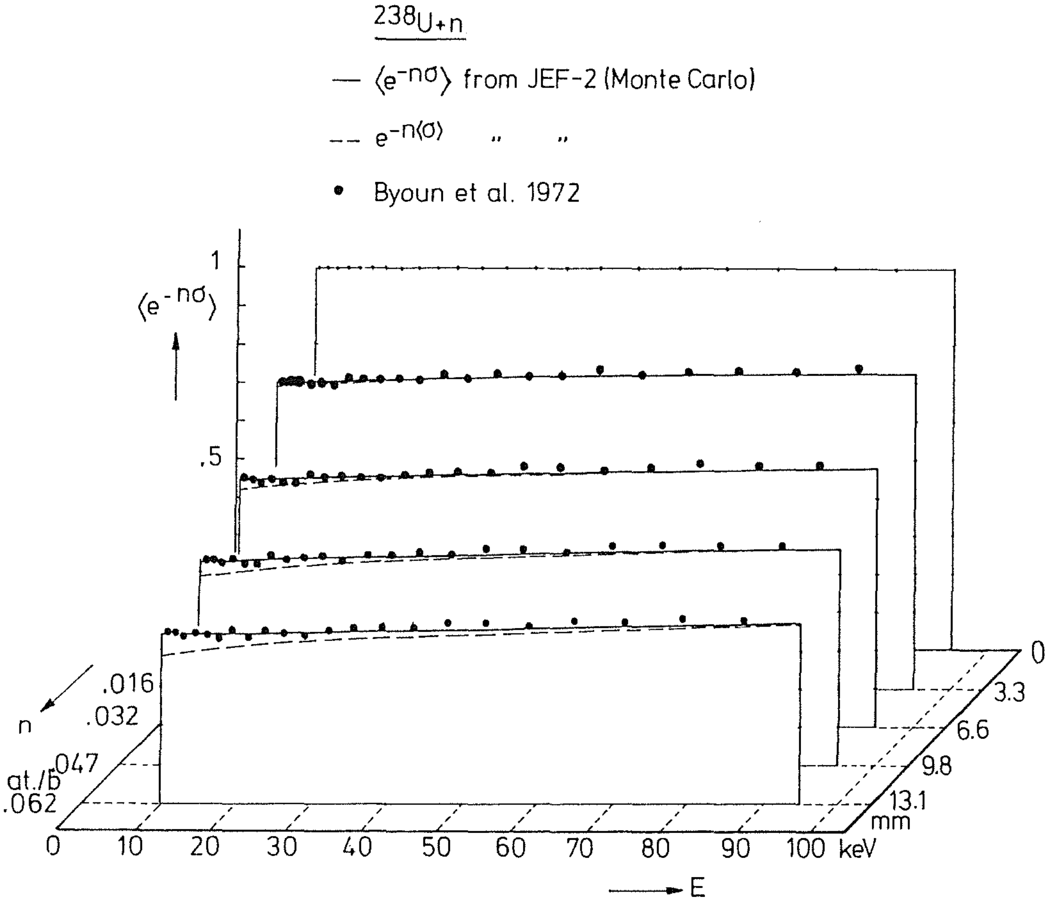

Fig. 5. Thick-sample transmission data of Byoun et al. (1972) (solid circles) and curves generated with Monte Carlo techniques from JEF-2 average resonance parameters (solid lines). Also shown are the transmission curves obtained with resonance self-shielding neglected (broken lines).

are the strength functions and distant-level parameters (or the effective nuclear radii). They determine, for the various partial waves, the ratio of compound (resonance) to direct (potential scattering) cross section. The thicker the sample, the more sensitive are the observed data to the cross section structure, the main weight being placed on the total cross section between resonances and, for thicker samples, on the resonance wings.

Doppler-broadened total cross sections were again sampled with the SESH program for the calculation of average transmission values corresponding to the extensive experimental data base established by Byoun et al. (1972), Bokhovko et al. (1988), and Grigoryev et

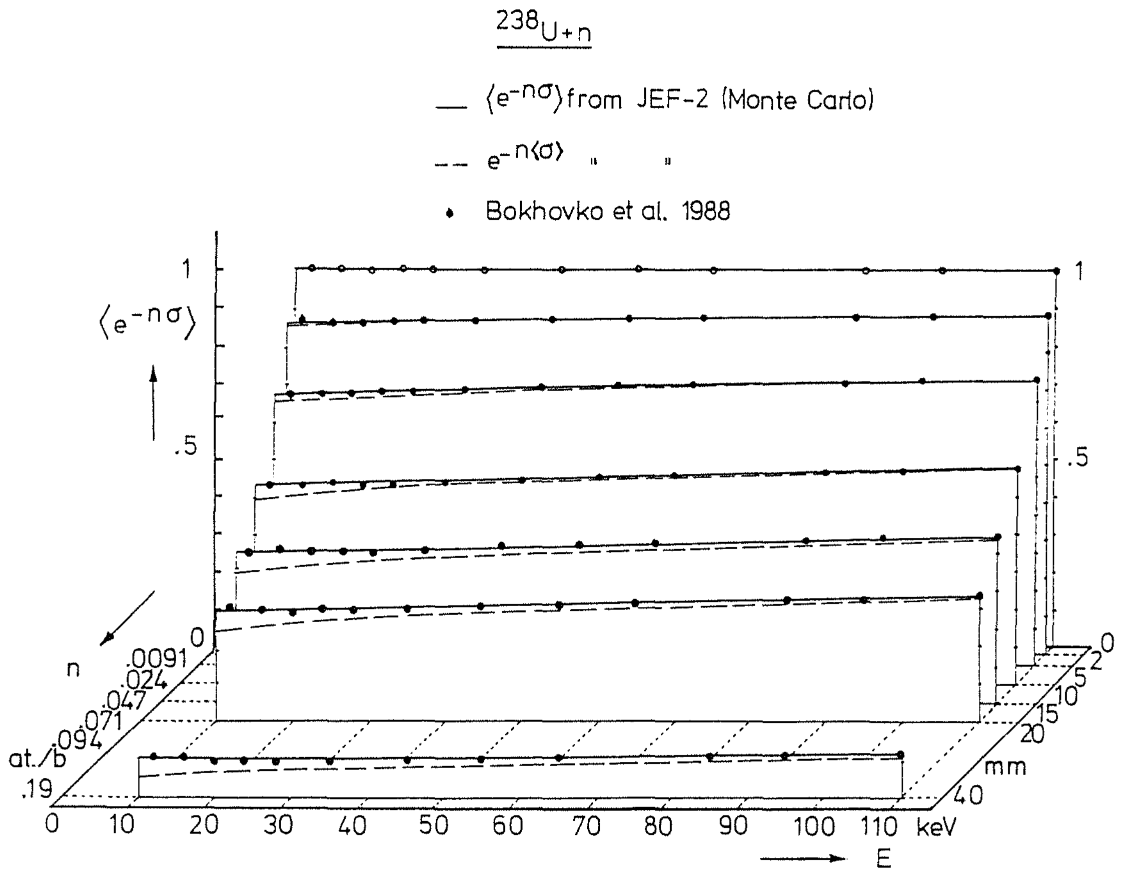

Fig. 6. Thick-sample transmission data of Bokhovko et al. (1988) (solid circles) and curves generated with Monte Carlo techniques from JEF-2 average resonance parameters (solid lines). Also shown are the transmission curves obtained with resonance self-shielding neglected (broken lines). Most error bars are slightly smaller than the point symbols.

al. (1990). Figs. 5 and 6 show a comparison with the most accurate measurements. The numbers plotted in Fig. 6 are listed in Table 1. Even for the thickest sample, corresponding to more than two mean free paths, the calculated values are seen to agree well with the experimental data, usually within the error bars. (Monte Carlo sampling was performed again with 100 000 neutron histories per initial energy to keep sampling errors well below 1 %). Comparable agreement was found with the data of Grigoryev et al. (1990). Thus the structure of the total cross section appears to be well represented by the average resonance parameters given in the new evaluation.

5. Comparison with Measured Self-Indication Ratios

Capture self-indication ratios are obtained if the transmitted part of the neutron beam

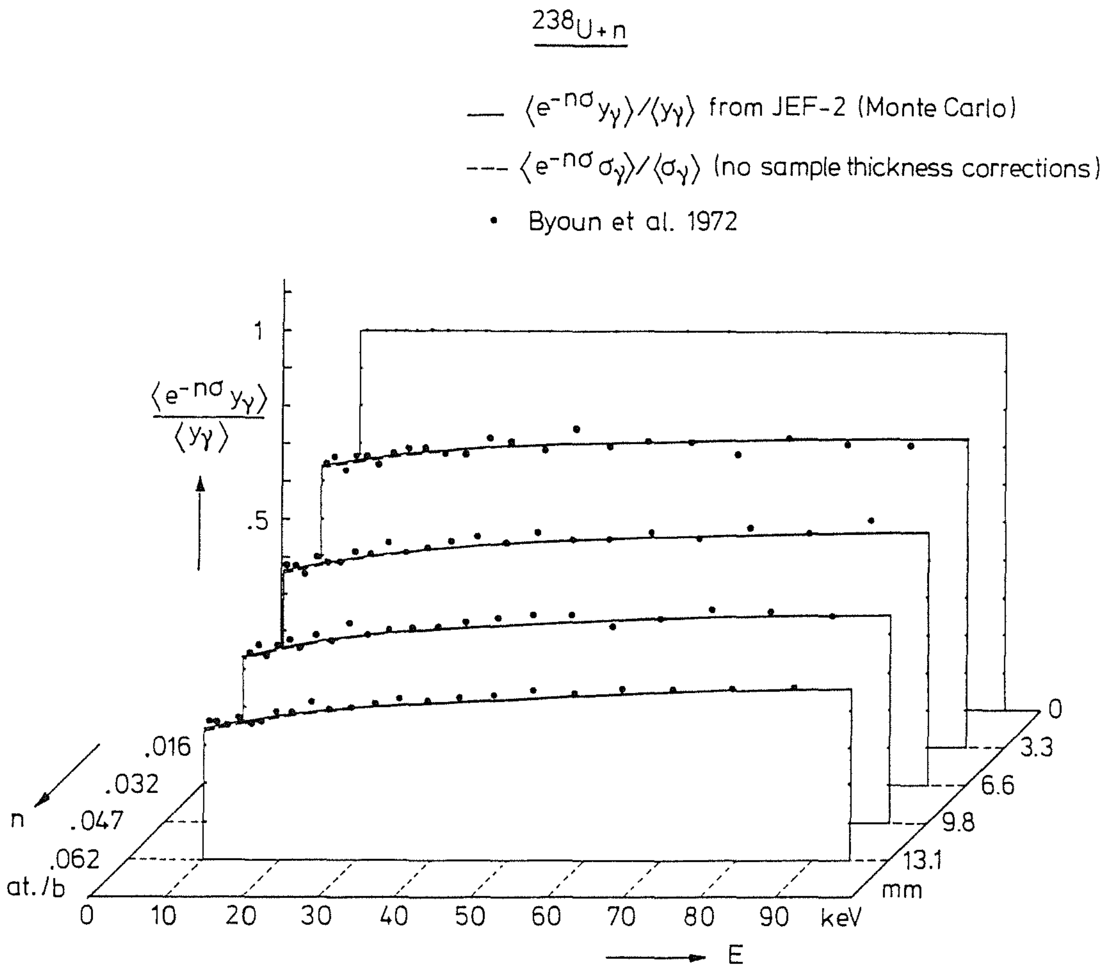

Fig. 7. Self-indication ratios measured by Byoun et al. (1972) (solid circles) and curves generated with Monte Carlo techniques from JEF-2 average resonance parameters (solid lines). Also shown are the results obtained without account for resonance self-shielding and multiple-collision capture, i. e. for vanishing radiator sample thickness (broken lines). The actual radiator sample thickness was 0.00376 at./b.

is allowed to undergo capture in a thin "indicator" sample (or "radiator") placed downstream of the filter sample, consisting of the same material, and viewed by gamma-ray detectors. From "filter in" and "filter out" runs one obtains the capture self-indication ratio, given by

$$\frac{\langle e^{-n\sigma}\sigma_\gamma\rangle}{\langle\sigma_\gamma\rangle} = e^{-n\langle\sigma\rangle}\left(1 - n\frac{\operatorname{cov}(\sigma,\sigma_\gamma)}{\langle\sigma_\gamma\rangle} + - \ldots\right) , \tag{3}$$

at least for a very thin radiator sample. Practical samples are not ideally thin, however, so the capture cross section σ_γ in this expression ought to be replaced by the capture yield y_γ that includes self-shielding and multiple-collision capture. In any case the self-

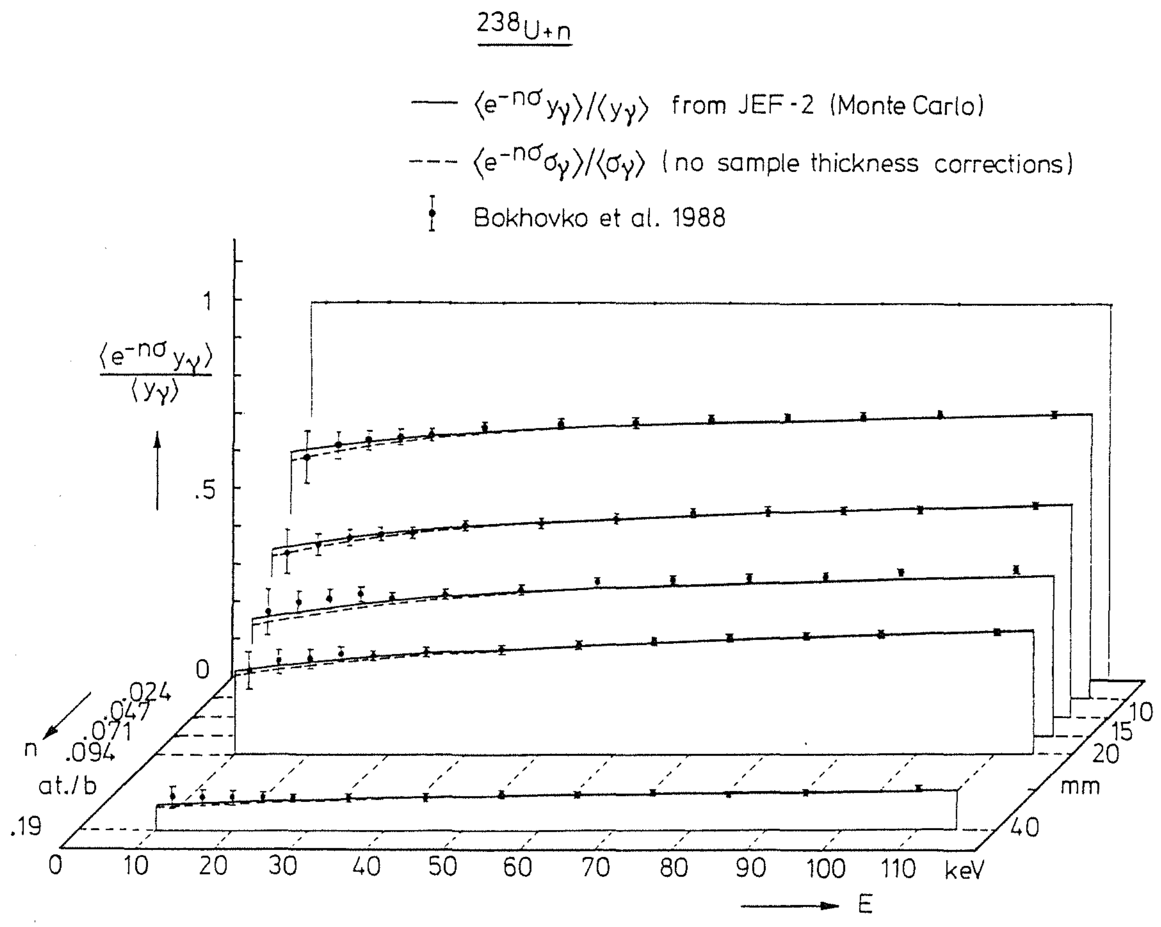

Fig. 8. Self-indication ratios measured by Bokhovko et al. (1988) (solid circles) and curves generated with Monte Carlo techniques from JEF-2 average resonance parameters (solid lines). Also shown are the results obtained without account for resonance self-shielding and multiple-collision capture, i. e. for vanishing radiator sample thickness (broken lines). The actual radiator sample thickness was 0.00646 at./b.

indication ratio depends on the total and the capture cross section and on their correlated resonance structure given by the covariance, $\mathrm{cov}(\sigma, \sigma_\gamma) = \langle(\sigma - \langle\sigma\rangle)(\sigma_\gamma - \langle\sigma_\gamma\rangle)\rangle$, and by higher mixed moments of the joint distribution of total and capture cross sections. As in transmission measurements the accuracy is inherently high since corrections to numerator and denominator tend to cancel at least partially while flux calibration and capture detector efficiency cancel exactly. The main weight is placed, however, on the peak regions, not on the regions between peaks as in transmission data, since self-indication ratios are essentially capture-weighted transmissions, and capture peaks coincide with transmission dips. Eq. 3 shows that the self-indication ratio depends only on the relative structure of the capture cross section but not on its absolute normalisation.

The SESH code was used again to calculate the observable ratio, $\langle e^{-n\sigma}y_\gamma\rangle/\langle y_\gamma\rangle$, from JEF-2 average resonance parameters. The results were compared with the data of Byoun et al. (1972), Bokhovko et al. (1988), and Grigoriev et al. (1990). None of these authors discusses sample thickness effects, i.e. the difference between capture cross section and capture yield, although the corrections are not negligible for some of the radiator samples used in the experiments. It is true that the corrections to numerator and denominator largely cancel, yet there may be a net effect of a few percent at low energies. Figs. 7 and 8 show the comparison of calculated and measured self-indication ratios, the latter being assumed to be uncorrected for sample thickness effects. A subset of the numbers plotted in Fig. 8 is shown in Table 2. Agreement is seen to be quite good, in particular with the very accurate data of Bokhovko et al. (1988), and the same is true for the data of Grigoriev et al. (1990). It is evident that not only the structure of the total cross section but also that of the capture cross section is well represented by the average resonance parameters given in the new ^{238}U evaluation.

6. Temperature Dependence of Thick-Sample Transmission

Byoun et al. (1972) provided thick-sample transmission values not only for room temperature, but also for sample temperatures of 77 K and 973 K, along with relevant information about thermal expansion of the two samples involved, and about the effective (Lamb-corrected) temperatures for Doppler broadening. The transmission of the cooled and heated samples could therefore be calculated with the SESH code from the total cross sections and average resonance parameters given in JEF-2. Table 3 contains a subset of the calculated results together with experimental values in the form of ratios (hot or cold transmission divided by room temperature transmission). Agreement is good. Similar agreement has been found for hot/cold transmission ratios calculated from the effective average total cross sections and thermal expansion data reported by Tsang and Brugger (1979) who used filtered neutron beams with 24 and 144 keV average energy and sample temperatures between 38 and 1100 K. Although their ratios agreed, the experimental transmission values themselves did not agree equally well with the calculated ones, hence the information from cooled and heated samples should not be overvalued. Doppler broadening tends to reduce the cross section structure and hence to decrease average transmission (see Eq. 2) while thermal expansion of the sample tends to increase it. Both effects amount to several percent and nearly compensate each other in the available data. Any conclusions about the resonance structure are therefore limited by uncertainties in the thermal expansion of the sample and in the effective temperatures describing crystal binding effects.

This is also true for measurements on thick uranium dioxide samples performed at 293, 1100 and 1800 K by Haste and Sowerby (1978, 1979). The room temperature transmission for one of their samples with n = 0.0942 U atoms/b can be directly compared with the data of Bokhovko et al. (1988) measured for a metallic uranium sample with 0.0943 atoms/b. The transmission of a stoichiometric dioxide sample should be smaller than that of the metallic sample by the factor $\exp(-2n\sigma) = 0.50$ for the known (smooth) oxygen cross section $\sigma = 3.73$ b at about 12 keV. Actually the data differ by a factor 0.58, which would imply an improbably low oxygen cross section of 2.9 b or a substoichiometric oxygen density. Moreover, the authors tried to circumvent explicit use of thermal expansion coefficients by an empirical correction that makes the reported cold/hot transmission ratios systematically too small.

In view of these difficulties it is concluded that at present the most stringent tests of the ^{238}U resonance structure are provided by room-temperature thick-sample transmission and self-indication data measured with metallic samples. They exhibit already a strong temperature effect, viz. Doppler broadening of natural line shapes to room temperature. Measurements with cooled and heated samples do not add much information because the change in Doppler broadening relative to room temperature is largely compensated by thermal expansion of the sample, with associated uncertainties.

7. Summary and Conclusions

Comparison of the newly evaluated average ^{238}U (n,γ) cross sections in the unresolved resonance region with recent capture yield data of Macklin et al. (1988) shows reasonable agreement if due account is taken of self-shielding and multiple-collision capture. A new absolute precision result, $\langle\sigma_\gamma\rangle = 494 \pm 11$ mb at 23 keV (Quang and Knoll 1990) is perfectly consistent with the recommended value $\langle\sigma_\gamma\rangle = 501$ mb at that energy in the new JEF-2 evaluation. In order to avoid misunderstanding it is stressed that these data are not considered preferable to the other published data known to the author. They are simply those that are not yet included in the evaluation itself, whereas the others (27 capture data sets, see Fröhner 1989) are utilised already and can therefore not serve as independent test material.

Monte Carlo generated average transmission values and self-indication ratios agree well with the extensive experimental data base provided by Byoun et al. (1972), Bokhovko et al. (1988), and Grigoriev et al. (1990). The agreement indicates that not only the absolute total and capture cross sections recommended in the JEF-2 evaluation are realistic but also the average resonance parameters specifying the resonance structure. The relative variation of average transmission with temperature as measured by Byoun et al. (1972) and by Tsang and Brugger (1979) is also satisfactorily reproduced, although the compensating effect and the uncertainties of thermal expansion makes these results somewhat less conclusive.

The consequences for self-shielding calculations can be seen from the relationship between self-shielding (Bondarenko) factors on one hand and average transmission values and self-indication ratios on the other,

$$f_\gamma = \frac{\langle\sigma_\gamma/(\sigma+\sigma_d)\rangle}{\langle\sigma_\gamma\rangle\,\langle 1/(\sigma+\sigma_d)\rangle} = \frac{\int_0^\infty dn\, e^{-n\sigma_d}\langle e^{-n\sigma}\sigma_\gamma\rangle/\langle\sigma_\gamma\rangle}{\int_0^\infty dn\, e^{-n\sigma_d}\langle e^{-n\sigma}\rangle}, \qquad (4)$$

where σ_d is the conventional (constant) dilution cross section of group constant sets and $\langle\ldots\rangle$ denotes group averages. It is evident that the possibility to predict $\langle e^{-n\sigma}\rangle$ and $\langle e^{-n\sigma}\sigma_\gamma\rangle/\langle\sigma_\gamma\rangle$ in a reliable way means that one can also predict f_γ reliably. The present results indicate that the new ^{238}U evaluation allows prediction of average transmission and self-indication ratios at room temperature with an accuracy of at least 1-2 % in the range of filter sample thicknesses n covered by the data (down to about 10 % transmission corresponding to more than two mean free paths). Because of the positive correlation between numerator and denominator in Eq. 4 it may thus be estimated that self-shielding factors can be computed with an accuracy of 0.5-1.5 %. At higher temperatures the resonances are Doppler broadened, hence the resonance structure is less pronounced and self-shielding factors differ less from unity, in other words temperature effects are less pronounced. It is therefore expected that self-shielding factors can be calculated for elevated temperatures at least as accurately as for room temperature.

The JEF-2 cross sections in the unresolved resonance range appear thus well supported by the microscopic data. Representing simultaneous Hauser-Feshbach fits to a large body of resonance-averaged total, capture and inelastic-scattering data, with rigorous GOE treatment of width fluctuation corrections and elastic enhancement (see Fröhner 1989), they are also consistent with the resolved-resonance data in JEF-2: The average s-wave parameters obtained in the fits, and given in the file for the unresolved resonance region, agree well with those extracted by validated missing-level estimation techniques (Fröhner 1989) from the resolved resonance parameters in the file (due to Moxon et al., 1988). Moreover, the s-, p-, d- and f-wave strength functions and distant-level parameters from the fits are consistent with those obtained from optical model calculations with, for instance, the spherical complex potential adjusted by Fischer (1980) to total cross sections and differential scattering data for ^{238}U (and other actinides) at higher energies, up to 15 MeV.

Finally, the JEF-2 capture cross sections in the unresolved resonance region agree well with three other recent evaluations: (i) with the pointwise, model-free evaluation of Poenitz (1988) performed as part of the comprehensive simultaneous evaluation of ENDB/B-VI standard cross sections, (ii) with the JENDL-3 evaluation that relies heavily on reactor experiments (Kanda et al. 1991), and (iii) with a new BROND evaluation (Blokhin et al. 1991). The mutual deviations between the four new capture cross section evaluations are less than 2 % between 10 and 200 keV.

All the tests against microscopic data indicate that the average (infinite-dilution) capture cross section of ^{238}U may now be known to about 1.5-2.5 % uncertainty between 10 and 200 keV, and that the associated self-shielding factors can be calculated with uncertainties of about 0.5-1.5 % . This comes close to the accuracies (1 σ uncertainties) requested for nuclear technology, in particular for reactor safety research, and for use as a secondary standard in neutron metrology (see WRENDA 87/88). In marked contrast, the accuracies presently achieved for the inelastic-scattering cross sections of $U238$ are still far below the requested ones.

ACKNOWLEDGMENTS. It is a pleasure to thank Dr. N.B. Janeva (Sofia, Bulgaria) for early communication of experimental results, Mrs. B. Krieg and Dr. I. Broeders for help with the NJOY calculations, and Dr. G. Schumacher for information about thermal expansion of uranium metal and oxides. Support by the German Nuclear Safety Research Project and by Prof. G. Kessler and Dr. H. Küsters is acknowledged.

Table 1. Thick-sample transmissions and uncertainties of Bokhovko et al. (1988) compared with Monte Carlo results based on JEF-2, as plotted in Fig. 6. Statistical uncertainties of Monte Carlo results are roughly 0.5 % .

E (keV)	Sample Thickness (at./b)					
	0.0091 (2 mm)	0.0237 (5 mm)	0.0474 (10 mm)	0.0707 (15 mm)	0.0943 (20 mm)	0.19 (40 mm)
10-14	0.884±0.006	0.718±0.005	0.525±0.009	0.398±0.008	0.299±0.005	0.104±0.005
	0.875	0.717	0.526	0.396	0.296	0.100
14-18	0.876±0.006	0.717±0.004	0.523±0.007	0.405±0.007	0.296±0.003	0.102±0.004
	0.878	0.719	0.532	0.398	0.295	0.099
18-22	0.880±0.004	0.719±0.004	0.531±0.006	0.400±0.005	0.288±0.002	0.093±0.003
	0.880	0.723	0.535	0.399	0.296	0.098
22-26	0.881±0.004	0.724±0.003	0.527±0.005	0.402±0.004	0.295±0.002	0.094±0.002
	0.882	0.725	0.535	0.401	0.296	0.097
26-30	0.881±0.004	0.722±0.003	0.527±0.006	0.398±0.004	0.292±0.002	0.093±0.002
	0.883	0.728	0.537	0.403	0.296	0.097
30-40	0.883±0.004	0.731±0.003	0.536±0.005	0.408±0.004	0.298±0.002	0.095±0.002
	0.885	0.732	0.541	0.407	0.301	0.098
40-50	0.887±0.004	0.739±0.003	0.540±0.004	0.417±0.004	0.304±0.002	0.099±0.002
	0.888	0.736	0.546	0.410	0.305	0.099
50-60	0.887±0.004	0.743±0.003	0.549±0.004	0.420±0.004	0.308±0.002	0.100±0.002
	0.890	0.740	0.551	0.416	0.309	0.101
60-70	0.893±0.004	0.748±0.003	0.554±0.004	0.425±0.004	0.316±0.002	0.103±0.002
	0.891	0.743	0.556	0.420	0.314	0.103
80-90	0.896±0.004	0.751±0.003	0.563±0.004	0.435±0.004	0.324±0.002	0.108±0.002
	0.894	0.749	0.564	0.429	0.322	0.108
90-100	0.899±0.004	0.757±0.003	0.565±0.003	0.440±0.003	0.328±0.002	0.110±0.002
	0.896	0.752	0.568	0.433	0.327	0.110
100-120	0.904±0.004	0.760±0.003	0.573±0.003	0.447±0.003	0.337±0.002	0.114±0.002
	0.898	0.756	0.574	0.439	0.333	0.114

Note: The interval 70-80 keV is missing from the table given by Bokhovko et al. (1988)

Table 2. Self-indication ratios and uncertainties of Bokhovko et al. (1988) compared with Monte Carlo results based on JEF-2, as plotted in Fig. 8. Statistical uncertainties of Monte Carlo results are roughly 0.5 % .

E	Sample Thickness (at./b)				
(keV)	0.0237 (5 mm)	0.0474 (10 mm)	0.0707 (15 mm)	0.0943 (20 mm)	0.19 (40 mm)
10-14	0.641±0.069	0.438±0.060	0.329±0.060	0.221±0.049	0.084±0.030
	0.654	0.455	0.317	0.229	0.065
18-22	0.683±0.025	0.477±0.021	0.363±0.024	0.254±0.025	0.085±0.017
	0.682	0.478	0.342	0.245	0.070
26-30	0.698±0.016	0.488±0.014	0.365±0.015	0.261±0.012	0.083±0.012
	0.696	0.495	0.357	0.260	0.076
40-50	0.726±0.014	0.511±0.012	0.390±0.011	0.279±0.010	0.084±0.010
	0.716	0.519	0.381	0.280	0.084
60-70	0.738±0.011	0.541±0.012	0.412±0.011	0.301±0.008	0.093±0.007
	0.728	0.538	0.400	0.295	0.092
80-90	0.745±0.010	0.544±0.009	0.422±0.009	0.316±0.008	0.094±0.006
	0.736	0.549	0.415	0.309	0.098
100-120	0.753±0.008	0.562±0.007	0.443±0.008	0.327±0.007	0.109±0.006
	0.751	0.565	0.431	0.324	0.102

Table 3. Thick-sample transmission ratios and uncertainties of Byoun et al. (1972) (transmission of cooled or heated sample relative to room temperature transmission, thermal expansion included) compared with Monte Carlo results based on JEF-2. Statistical uncertainties of Monte Carlo results are roughly 0.7 % .

Energy Range (keV)	Temperature Ratio (K : K)	Sample Thickness (at./b) 0.03155 (6.6 mm)	Sample Thickness (at./b) 0.06206 (13.1 mm)	Temperature Ratio (K : K)	Sample Thickness (at./b) 0.03155 (6.6 mm)	Sample Thickness (at./b) 0.06206 (13.1 mm)
15.2-16.8	77:293	1.005±0.012	1.010±0.011	973:293	1.026±0.018	1.010±0.011
		1.007	1.018		1.018	0.992
22.6-25.0		1.007±0.012	0.999±0.012		1.029±0.012	1.011±0.012
		1.005	1.019		1.022	0.998
33.8-37.3		0.999±0.013	1.008±0.013		1.026±0.013	1.016±0.013
		1.003	1.010		1.023	1.005
50.4-55.7		0.997±0.013	1.004±0.012		1.029±0.012	1.023±0.013
		1.002	1.011		1.024	1.007
83.1-91.9		0.998±0.015	0.992±0.014		1.023±0.014	1.021±0.015
		1.001	1.003		1.023	1.023

REFERENCES

A.I. Blokhin, A.V. Ignatyuk, B.D. Kuzminov, V.N. Manokhin, G.N. Manturov and M.N. Nikolaev, Proc. Internat. Conf. on Nucl. Data in Sci. and Technol., Jülich, 1991 (in print); B.D. Kuzminov, private communication (1991)

M.V. Bokhovko, V.N. Kononov, G.N. Manturov, E.D. Poletaev, V.V. Sinitsa and A.A. Voevodskij, Yad. Konst. **3** (1988) 11; Engl. transl. INDC(CCP)-322 (1990) p. 5

T.Y. Byoun, R.C. Block and T. Semler, Proc. Kiamesha Lake Conf. 1972, CONF-720901, Book 2, p. 1115 (1972)

G. de Saussure and R.B. Perez, Nucl. Sci. Eng. **52** (1973) 382

F.H. Fröhner, General Atomic Report GA-8380 (1968)

F.H. Fröhner, Nucl. Sci. Eng. **102** (1989) 119 (note: the ordinate numbers in Fig. 3 are too high by a factor of 10)

A. Gilbert and A.G.W. Cameron, Can. J. Physics **43** (1965) 1446

Yu.V. Grigoriev, V.N. Koshcheev, G.N. Manturov, I.A. Sirakov, V.V. Sinitsa, N.B. Janeva, Obninsk Report FEI-2072 (1990)

T.J. Haste and M.G. Sowerby, Harwell Report AERE-R 8961 (1978);

T.J. Haste and M.G. Sowerby, J. Phys. D: Appl. Phys. **12** (1979) 1203

Y. Kanda, Y. Kikuchi, Y. Nakajima, M.G. Sowerby, M.C. Moxon, F.H. Fröhner, W.P. Poenitz and L.W. Weston, Proc. Internat. Conf. on Nucl. Data in Sci. and Technol., Jülich, 1991 (in print)

K. Kobayashi, S. Yamamoto and Y. Fujita, Proc. Internat. Conf. on Nucl. Data in Sci. and Technol., Jülich, 1991 (in print)

R.E. MacFarlane, Proc. Seminar on NJOY and Themis, OECD Paris (1989) p. 7

Roger L. Macklin, R.B. Perez, G. de Saussure and R.W. Ingle, Proc. Int. Conf. Nucl. Data for Sci. and Technol., Mito 1988, ed. S. Igarasi, Tokyo (1988) p. 75

M. Moxon, M. Sowerby, Y. Nakajima and C. Nordborg, Proc. Internat. Reactor Physics Conf., Jackson Hole, ANS (1988), vol. I, p. 281

C. Nordborg, H. Gruppelaar and M. Salvatores, Proc. Internat. Conf. Nucl. Data for Sci. and Technol., Jülich 1991, in print

W.P. Poenitz, private communication (1988)

C.E. Porter, ed., "Statistical Theory of Spectra: Fluctuations", Acad. Press, New York and London (1965)

E. Quang and G. Knoll, Trans. Am. Nucl. Soc. **61** (1990) 399

F.Y. Tsang and R.M. Brugger, Nucl. Sci. Eng. **72** (1979) 52

J.M. Verbaarschot, H.A. Weidenmüller and M.R. Zirnbauer, Phys. Repts. **129** (1985) 367

WRENDA 87/88, World Request List for Nuclear Data, ed. Wang Dahai, IAEA Report INDC(SEC)-95/URSF, Vienna (1988)